Antibody Targeting of Long-Circulating Lipidic Nanoparticles Does Not Increase Tumor Localization but Does Increase Internalization in Animal Models

Dmitri B. Kirpotin,[1,2] Daryl C. Drummond,[1,2] Yi Shao,[2] M. Refaat Shalaby,[2] Keelung Hong,[1,2] Ulrik B. Nielsen,[3] James D. Marks,[3] Christopher C. Benz,[4] and John W. Park[4]

[1]Hermes Biosciences, Inc., South San Francisco; [2]California Pacific Medical Center Research Institute; [3]Department of Anesthesia, and [4]Division of Hematology-Oncology, University of California, San Francisco, San Francisco, California

Abstract

We describe evidence for a novel mechanism of monoclonal antibody (MAb)–directed nanoparticle (immunoliposome) targeting to solid tumors *in vivo*. Long-circulating immunoliposomes targeted to HER2 (ErbB2, Neu) were prepared by the conjugation of anti-HER2 MAb fragments (Fab′ or single chain Fv) to liposome-grafted polyethylene glycol chains. MAb fragment conjugation did not affect the biodistribution or long-circulating properties of i.v.-administered liposomes. However, antibody-directed targeting also did *not* increase the tumor localization of immunoliposomes, as both targeted and nontargeted liposomes achieved similarly high levels (7-8% injected dose/g tumor tissue) of tumor tissue accumulation in HER2-overexpressing breast cancer xenografts (BT-474). Studies using colloidal gold-labeled liposomes showed the accumulation of anti-HER2 immunoliposomes within cancer cells, whereas matched nontargeted liposomes were located predominantly in extracellular stroma or within macrophages. A similar pattern of stromal accumulation without cancer cell internalization was observed for anti-HER2 immunoliposomes in non–HER2-overexpressing breast cancer xenografts (MCF-7). Flow cytometry of disaggregated tumors posttreatment with either liposomes or immunoliposomes showed up to 6-fold greater intracellular uptake in cancer cells due to targeting. Thus, in contrast to nontargeted liposomes, anti-HER2 immunoliposomes achieved intracellular drug delivery via MAb-mediated endocytosis, and this, rather than increased uptake in tumor tissue, was correlated with superior antitumor activity. Immunoliposomes capable of selective internalization in cancer cells *in vivo* may provide new opportunities for drug delivery. (Cancer Res 2006; 66(13): 6732-40)

Introduction

Targeted delivery of anticancer drugs to tumors has been long sought to improve the therapeutic index of cancer treatment. Liposomes represent a now well-established strategy for drug delivery, and have entered clinical use after years of optimization. Although the first generation of liposomes was limited by modest drug encapsulation efficiencies and rapid clearance by the reticuloendothelial system, progressive optimization has resulted in more stable and long-circulating liposomes with increased deposition in tumors (1, 2), which provide potential clinical benefits in certain cases. The next generation of nanoparticle-based drug delivery systems includes immunoliposomes, in which antibody fragments are conjugated to long-circulating liposomes for targeted drug delivery (for review, see ref. 3).

We have previously described anti-HER2 immunoliposomes, in which sterically stabilized liposomes containing polyethylene glycol (PEG) were conjugated to monoclonal antibody (MAb) fragments specific for the HER2 (ErbB2, Neu) oncoprotein (4, 5). Anti-HER2 immunoliposomes selectively bind to and internalize in HER2-overexpressing cancer cells *in vitro* via receptor-mediated endocytosis, thus potentially providing a vehicle for intracellular drug delivery (5, 6). Doxorubicin-loaded anti-HER2 immunoliposomes produced marked therapeutic results in HER2-overexpressing xenograft models, and were significantly superior to all other treatment conditions tested, including free doxorubicin, nontargeted liposomal doxorubicin, recombinant anti-HER2 MAb trastuzumab, and combinations of these other agents (4).

Here, we provide experimental evidence for the mechanisms underlying this increased antitumor efficacy, and show that it does not involve enhanced accumulation of anti-HER2 immunoliposomes in tumor tissue due to antigen binding. Rather, both liposomes and immunoliposomes localized at high levels in tumor tissue, but revealed a marked difference in pharmacodynamics with respect to tumor cells *in vivo*: immunoliposomes, but not liposomes, mediated intracellular drug delivery to HER2-overexpressing cancer cells in animal models.

Materials and Methods

Liposome and immunoliposome preparations. The liposome matrix was phosphatidylcholine (Avanti Polar Lipids, Alabaster, AL), cholesterol (Calbiochem, San Diego, CA), and *N*-methoxy-PEG (molecular weight, 1,900)-oxycarbonyl-distearoylphosphatidylethanolamine (DSPE; Genzyme, Cambridge, MA) as previously described (4). MAb fragments consisted of either Fab′ fragments, rhuMAbHER2-Fab (7), from recombinant humanized anti-HER2 MAb trastuzumab (Genentech, Inc., South San Francisco, CA), or human anti-HER2 single chain Fv (scFv) F5 with COOH-terminal cysteine (8–11). The linker was *N*-[α-(2-[*N*′-maleimido]propyonylamido)-PEG-omega-oxycarbonyl]-DSPE (6, 10, 11). PEG chains had a molecular weight of 2,000. For biodistribution and tissue microdistribution studies, immunoliposomes were prepared as previously described (6), including a linker at 2 mol% of liposomal phospholipid, and conjugation to recombinant anti-HER2 Fab′ derived from trastuzumab; Fab′ density was ~33 Fab′/immunoliposome. For flow cytometry studies, immunoliposomes were prepared by micellar incorporation of anti-HER2 scFv F5 as previously described (10, 11). The final linker concentration, including F5-conjugated and residual unconjugated (cysteine-quenched) linker was ~0.2 mol% of the liposomal phospholipid; scFv density was ~20 scFv/immunoliposome. Unused linker

Requests for reprints: John W. Park, San Francisco Comprehensive Cancer Center, University of California, 1600 Divisadero Street, 2nd Floor, San Francisco, CA 94115. Phone: 415-502-3844; Fax: 415-353-9592; E-mail: jpark@cc.ucsf.edu.

doi:10.1158/0008-5472.CAN-05-4199

was cysteine-quenched in all liposomes where present. Liposome/immunoliposome size was 90 to 110 nm by dynamic light scattering.

For radiolabeling, ^{67}Ga (1.0-1.5 μCi/μmol phospholipid) was loaded into liposomes and immunoliposomes containing 95 mmol/L of sodium diethylenetriamine pentaacetate (DTPA; pH 5.5) using USP diagnostic grade (^{67}Ga)-gallium citrate (12). Encapsulation of colloidal gold was done as described (13); to facilitate the entrapment of gold chloride solution, liposomes were prepared with egg phosphatidylcholine and reverse-phase evaporation (14), and MAb fragments were conjugated following gold encapsulation. Liposomes containing water-soluble fluorescent marker, ADS645WS (American Dye Source, Inc., Quebec, Canada), were prepared with hydration of the neat lipid matrix of DSPC, cholesterol, and PEG-DSPE (3:1:1 by weight) in 5 mmol/L dye solution in normal saline, followed by sequential membrane extrusion and Sepharose CL-4B (GE Healthcare, Piscataway, NJ) chromatography to remove the unencapsulated dye. The mean nanoparticle size was 86 nm. Immunoliposomes were prepared from ADS645WS-loaded liposomes by coincubation with a micellar solution of F5-maleimide-PEG-DSPE conjugate at a ratio of 10 μg protein/μmol liposomal phospholipid (9–11). ADS645WS-loaded nanoparticles were concentrated in a stirred ultrafiltration cell on an Amicon YM100 membrane (Millipore, Billerica, MA) to reach a concentration of 40 to 44 mmol/L of phospholipid. Liposomal phospholipid concentration was determined by phosphate assay (15). Conjugated protein was assayed by the dye-binding method (Bio-Rad Laboratories, Hercules, CA) and SDS-PAGE with Coomassie blue staining and spectrophotometry of the 49 kDa band at 595 nm. The HER2-specific reactivity of radiolabeled immunoliposomes was confirmed in cultured SK-Br-3 cells (0.2 mmol/L liposome phospholipid after 4 hours of incubation at 37°C).

Tumor and tissue uptake of lipidic nanoparticles in mice. Tumor cells (2×10^7; BT-474 or MCF-7) were inoculated s.c. in the upper back of 4- to 6-week-old female NCR homozygous nude mice, with sustained-release 17β-estradiol pellets (Innovative Research of America, Sarasota, FL) implanted in the lower back, and allowed to grow for 10 to 14 days postinoculation. Studies included 54 animals with tumors ranging from 220 to 1,200 mm^3 (median, 450 mm^3). For each agent (HER2-targeted or nontargeted), animals were randomly assigned to nine groups of three animals each, corresponding to time points of 4, 8, 12, 24, 48, 72, 99, 123, and 168 hours postinjection. Liposomes with encapsulated ^{67}Ga-DTPA were injected via tail vein at 40 μmol phospholipid/kg of body weight. At the indicated times, the animals were anesthetized, exsanguinated via open heart puncture, and perfused through the left ventricle. Blood, tumor, and other tissues were collected and weighed; liposome levels were determined by radioactivity counting, and corrected for radioactive decay. The total injected dose was calculated from the injection volume and specific activity of the liposome/immunoliposome preparations measured simultaneously with tissue samples. Linear regression analysis did not show significant correlation between liposome uptake (expressed as the percentage of injected dose per gram of tissue) versus tumor size, which was consistent with previous observations (16).

Microdistribution of lipidic nanoparticles within tumor tissue. Colloidal gold-labeled liposomes/immunoliposomes were injected i.v. into tumor-bearing mice at a dose of 0.4 mmol phospholipid/kg. Results represent six separate experiments in BT-474 or MCF-7 models and a total of 24 animals. Tumor volumes ranged from 100 to 700 mm^3. Forty-eight hours later, animals were sacrificed; tumors were fixed overnight with 4% formaldehyde in PBS, embedded in glycol methacrylate, and cut into 3-μm sections. Sections were made serially through multiple regions of each tumor (4, 5), excluding grossly necrotic areas, followed by silver enhancement using the Aurion R-Gent kit (Electron Microscopy Sciences, Fort Washington, PA) and light staining with H&E. To avoid artifacts, the silver-enhancement time was adjusted to prevent the appearance of silver grains in the tissue-free section area and on the concurrently enhanced sections of blank (liposome-free) tumors. Sections were examined using bright-field and dark-field microscopy. At low power magnifications, light-reflective silver staining was visualized by side illumination using the Darklite fiber optic illuminator (Micro Video Instruments, Avon, MA). Observations from tumor-to-tumor and section-to-section varied somewhat in terms of total liposome/immunoliposome accumulation, but were consistent as to tumor cell versus stromal partitioning. Representative micrographs are shown in Results.

Quantitative analysis of immunoliposome/liposome uptake in tumor cells *in vivo*. ADS645WS-loaded nontargeted liposomes or F5-conjugated immunoliposomes were injected i.v. into mice bearing BT-474 s.c. tumors (360-600 mm^3; four animals per group) at 0.4 mmol phospholipid/kg. Nontreated animals provided tumors that served as controls. Forty-four hours later, animals were sacrificed by cervical dislocation, and tumors were excised, mechanically fragmented, and treated sequentially with two portions of disaggregation solution [0.1% collagenase type IV (Sigma Chemical Co., St. Louis, MO) and 0.003% DNase I in Hank's buffered salt solution] for 20 minutes at 37°C with slow agitation. Following centrifugation at 4°C, cell pellets were gently resuspended in cold PBS containing 0.1% bovine serum albumin (BSA; type V, Sigma) and 0.02% sodium azide (BSA-PBS-azide). To differentiate cancer cells from cells of the mouse host, the cell suspension was stained with FITC-conjugated mouse MAb against human epithelial antigen (HEA125; Miltenyi Biotec, Auburn, CA) on ice for 15 minutes. The cells were diluted with cold BSA-PBS-azide, centrifuged and resuspended in BSA-PBS-azide, and centrifuged again. After three washes, cells were resuspended in PBS, fixed with paraformaldehyde (0.9% final concentration), and strained through a 53-μm nylon mesh. Flow cytometry was done (FACSCalibur, BD Biosciences, San Jose, CA) using the fluorescein (FL1) channel for HEA-FITC and Cy5 (FL-4) channel for liposomal ADS645WS. Cultured BT-474 cells served as a positive control for HEA staining. Ten thousand scatter-gated signals were collected per sample.

To verify intracellular localization of particles, cell suspensions were examined with a Nikon T2000 inverted confocal microscope employing FITC and Cy5 detection laser-filter sets for visualization of HEA and liposomes, respectively.

Cytochemical identification of tissue macrophages. Glycol methacrylate–embedded tissue sections +/− silver enhancement were stained for nonspecific (α-naphtyl acetate) esterase using a commercial kit (91-A, Sigma), except that Fast Violet Red LB was substituted for Fast Blue BB to afford nonoverlapping colors between the esterase reaction (violet) and black silver grains signifying liposome localization. Sections were counterstained in Gill's hematoxylin no. 3, mounted in crystal/mount (Biomeda, Foster City, CA), and examined by microscopy. There was no difference in pigment localization in sections stained before or after the silver enhancement step.

Results

Design of anti-HER2 immunoliposomes. Anti-HER2 immunoliposomes were produced by covalent conjugation of recombinant MAb fragments to sterically stabilized/pegylated liposomes. Liposomes consisted of small (80-100 nm) unilamellar vesicles containing phosphatidylcholine, cholesterol, PEG (molecular weight, 2,000)–modified PEG-DSPE, and maleimide-terminated PEG-DSPE to afford covalent conjugation of MAb fragments to the termini of surface-grafted PEG chains ("PEG-MAb linkage"; ref. 6). Conjugation was very efficient (>90% of added MAb fragment) and yielded high ligand density (>20 MAb fragment per immunoliposome). As controls, nontargeted pegylated liposomes were prepared identically except for the omission of MAb fragment conjugation.

Anti-HER2 MAb fragments included either Fab′ derived from recombinant humanized MAb trastuzumab (17) or scFv F5, isolated via phage antibody screening for internalization in target cells (8). Immunoliposomes containing these or other MAb fragments have not shown any significant differences in pharmacokinetic properties (ref. 4, 18; data not shown). Whether constructed with trastuzumab-derived Fab′ (4) or scFv F5 (9), anti-HER2 immunoliposomal doxorubicin showed superior antitumor efficacy over nontargeted liposomal doxorubicin in HER2-overexpressing tumor models *in vivo*.

Table 1. Biodistribution of radiolabeled HER2-targeted and nontargeted sterically stabilized liposomes in nontumor tissues 24 hours post-i.v. injection

Tissue	Liposome uptake, injected dose/g tissue (%)	
	Nontargeted sterically stabilized liposomes	Anti-HER2 immunoliposomes
Blood	7.98 ± 0.85	7.04 ± 0.82
Liver	14.2 ± 1.9	15.6 ± 3.8
Spleen	33.5 ± 5.5	41.6 ± 4.7
Kidneys	3.72 ± 0.24	3.21 ± 0.24
Lungs	0.61 ± 0.10	0.42 ± 0.1
Heart	0.68 ± 0.16	0.58 ± 0.05
Skin	3.97 ± 0.72	4.71 ± 0.86
Muscle	0.74 ± 0.20	0.37 ± 0.12
Bone	3.50 ± 0.82	2.06 ± 0.35

NOTE: Mice with 200 to 300 mm^3 s.c. tumor xenografts received a single i.v. injection of liposomes or anti–HER2-Fab′-conjugated immunoliposomes containing encapsulated ^{67}Ga-DTPA (4 μmol liposomal phospholipid/kg). Twenty-four hours later, animals were sacrificed and tissue radioactivity was determined (Materials and Methods). Total recovery of label >80% of calculated. Data represent mean ± SD (five animals/group).

Biodistribution of anti-HER2 immunoliposomes. Radiolabeled liposomes and anti-HER2 immunoliposomes were prepared by the encapsulation of ^{67}Ga-DTPA chelate, which is essentially membrane-impermeable and released only on breakdown of liposomes in tissues; once released, ^{67}Ga-DTPA is then rapidly excreted (12). We have reported that liposomes containing encapsulated ^{67}Ga-DTPA display essentially identical pharmacokinetics to cognate liposomes containing doxorubicin (4). This pharmacokinetic profile differs markedly from that of free Gd chelates, including Ga-DTPA, and rules out any significant Ga or Ga-DTPA release from liposomes during circulation. Furthermore, even if any released Ga were subject to transchelation such as to transferrin, the pharmacokinetics of liposome-encapsulated ^{67}Ga-DTPA corresponds to that of the liposomes themselves ($t_{1/2}$, 12-16 hours or more; ref. 4) and not to Ga-transferrin complexes ($t_{1/2\beta}$, ~140 minutes; refs. 15, 19). Thus, liposome-encapsulated ^{67}Ga-DTPA provides an ideal *in vivo* marker for liposomal drug. A dose of 40 μmol phospholipid/kg was used in the biodistribution studies as it is equivalent to the therapeutic dose used in antitumor efficacy studies of liposomal versus immunoliposomal doxorubicin, which showed increased efficacy for immunoliposome treatment (4).

Twenty-four hours after i.v. injection, both anti-HER2 immunoliposomes and nontargeted liposomes distributed to comparable levels in all of the sampled normal tissues (Table 1). Immunoliposomes displayed a biodistribution pattern characteristic of long-circulating liposomes (20), including reduced reticuloendothelial uptake and high blood concentrations. It is notable that the presence of MAb fragments on immunoliposomes did not result in any apparent alteration of liposome biodistribution or pharmacokinetics. These results are consistent with the plasma pharmacokinetics previously observed for anti-HER2 immunoliposomes in normal adult rats, in which immunoliposomes and sterically stabilized liposomes displayed equally long circulation times (4).

Tumor localization of anti-HER2 immunoliposomes versus nontargeted liposomes. Increased tumor localization of MAbs and immunoconjugates has long been considered a paradigm for antibody-based cancer treatments. Because both MAbs and liposomes accumulate in tumors, we carefully evaluated the tumor localization of anti-HER2 immunoliposomes, including direct comparisons with nontargeted liposomes in HER2-overexpressing tumors following i.v. administration. Importantly, the anti-HER2 MAb–mediated targeting of immunoliposomes did not increase tumor accumulation over that of nontargeted sterically stabilized liposomes (Table 2). Both anti-HER2 immunoliposomes and nontargeted liposomes showed efficient localization in breast tumor xenografts: liposome levels reached 7% to 8% injected dose/g tumor tissue whether MAb fragments were present or not, and whether the tumor was HER2-overexpressing (BT-474) or not (MCF-7).

Some MAb/ligand-directed liposomes have been reported to provide prolonged retention in tumor tissue (21), suggesting increased tumor exposure to liposomal drug, and therefore increased efficacy. We evaluated the kinetics of liposome and anti-HER2 immunoliposome accumulation in tumors for 7 days postinjection (Fig. 1*A*). The time course of tumor concentration was largely identical for nontargeted liposomes and immunoliposomes. In both cases, tumor levels increased during the initial 24 hours postinjection, remained at high levels until 72 hours, and then slowly declined thereafter, with >1% injected dose/g of tumor tissue still remaining after 7 days. Although tumor levels of immunoliposomes were somewhat higher than those of nontargeted liposomes at certain time points, these differences were not significantly different ($P > 0.05$, two-tailed unpaired Student's t test) with the exception of a single time point (120 hours). We did not observe any significant label washout in these studies. As noted, the pharmacokinetic profile of liposome-encapsulated ^{67}Ga-DTPA seen here corresponds closely to that of liposomal and immunoliposomal doxorubicin in our previous studies (4), indicating highly stable encapsulation of marker or drug while circulating. The cellular metabolism of Gd-DTPA was not examined.

Table 2. Uptake of radiolabeled nontargeted liposomes and anti-HER2 immunoliposomes in breast tumor xenografts 24 hours post-i.v. injection

Tumor	Liposome uptake, injected dose/g tissue (%)		*P*
	Nontargeted sterically stabilized liposomes	Anti-HER2 immunoliposomes	
BT-474	7.32 ± 1.05	8.34 ± 1.54	0.256
MCF-7	8.59 ± 2.32	7.18 ± 1.04	0.376
BT-474 tumor/muscle	9.9	22.5	
MCF-7 tumor/muscle	11.6	19.4	

NOTE: For details, see Table 1. *P*, probability of the null hypothesis by the independent two-tailed t test, targeted versus nontargeted liposomes.

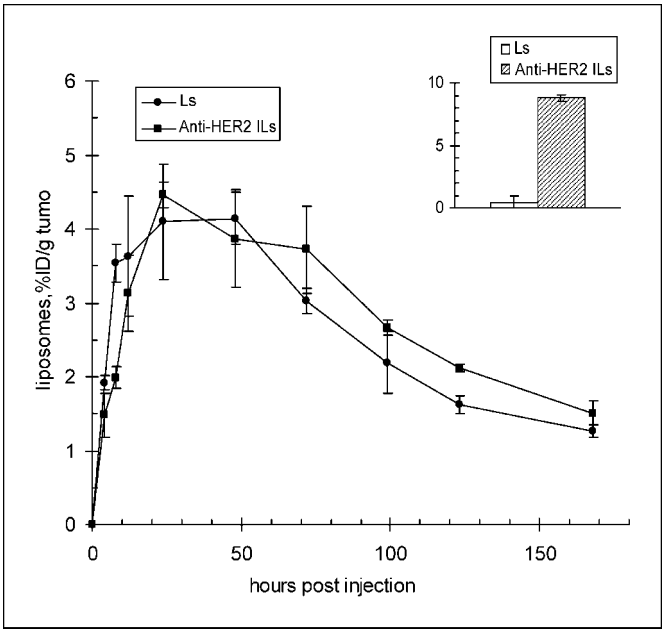

Figure 1. Tumor pharmacokinetics of ^{67}Ga-labeled anti-HER2 immunoliposomes (Fab′ targeted) versus control pegylated liposomes (*Ls*) in s.c. BT-474 breast cancer xenografts in nude mice. Liposomes/immunoliposomes were administered i.v. at 40 μmol phospholipid/kg. *Points,* mean; *bars,* ±SD; three animals per group. *Inset,* uptake of anti-HER2 immunoliposomes (*cross-hatched column*) versus control liposomes (*solid column*) in HER2-overexpressing breast cancer cells (SK-Br-3) *in vitro*. Uptake units, nmol liposome phospholipid/10^6 cells (mean ± SD; n = 4 experiments).

As a positive control for the targeting effect *in vitro*, the same preparation of anti-HER2 immunoliposomes showed markedly greater uptake in cultured HER2-overexpressing breast cancer cells than nontargeted liposomes (Fig. 1, *inset*).

Doxorubicin-loaded anti-HER2 immunoliposomes showed significantly greater antitumor efficacy than nontargeted liposomal doxorubicin in this same BT-474 tumor model (4, 9), as well as in other HER2-overexpressing models (4). Yet, anti-HER2 immunoliposomes at equivalent doses failed to show increased accumulation or retention in tumor tissue compared with their nontargeted counterparts, thus ruling out increased tumor localization as the mechanism responsible for the therapeutic advantage of immunoliposome delivery.

Intratumoral distribution of anti-HER2 immunoliposomes versus nontargeted liposomes. This paradox was further investigated in detailed analyses of liposomes and immunoliposomes within tumor tissue, which revealed fundamental differences in microdistribution and cellular localization for anti-HER2 immunoliposomes in HER2-overexpressing tumors versus their nontargeted counterparts. As previously reported, anti-HER2 immunoliposomes undergo receptor-mediated endocytosis in target cells *in vitro*, resulting in intracellular delivery of encapsulated agents, whereas nontargeted liposomes do not bind or internalize in these cells (5, 6). To evaluate the distribution of these particles within tumor tissue following i.v. administration, anti-HER2 immunoliposomes or matching nontargeted liposomes labeled with encapsulated colloidal gold were administered i.v. in nude mice bearing BT-474 or MCF-7 tumors. Microdistribution studies using gold or fluorescently labeled liposomes/immunoliposomes employed a dose of 0.4 mmol/kg, which was higher than that used in biodistribution and therapy studies in order to achieve greater signal. Forty-eight hours postinjection, tumors were harvested and immunoliposomes/liposomes were visualized in tumor sections by light microscopy following silver enhancement (13).

Low-power magnification microscopy of BT-474 tumors showed that both nontargeted liposomes and anti-HER2 immunoliposomes had extravasated in large amounts from tumor vessels (Fig. 2*A* and *B*), consistent with the high tumor levels previously measured. Both nanoparticles were observed in areas of apparently viable tumor tissue, in necrotic regions, and particularly at the interface between these regions—a zone often associated with high local concentrations of angiogenic and permeability factors and consequent neovascularization (22, 23). Tumor penetration of liposomes and immunoliposomes clearly exceeded the predominantly perivascular deposition often reported with liposomes in other studies (24, 25); furthermore, a "binding site barrier" phenomenon described for some tumor cell–specific antibodies (28) was not observed for anti-HER2 immunoliposomes. At intermediate magnification of BT-474 tumor tissue, immunoliposome localization seemed to be qualitatively different from that of liposomes. Whereas immunoliposomes were distributed throughout tumor tissue in close association with tumor cells (Fig. 2*C* and *D*), nontargeted liposomes showed a more uneven or patchy distribution, with high focal accumulation within tumor stroma and less association with tumor cells (Fig. 2*E* and *F*).

At high-power magnification, anti-HER2 immunoliposomes were predominantly detected within tumor cells, as evidenced by silver grains in tumor cell cytoplasms (Fig. 3*A*). Internalized immunoliposomes were often concentrated in the perinuclear region of the cytoplasm, consistent with our previous observations in HER2-overexpressing cells *in vitro* (5, 6). In contrast, nontargeted liposomes accumulated predominantly within tumor stroma, either in the extracellular space or within tumor-resident macrophages (Fig. 3*B*). This extracellular and macrophage disposition is consistent with previous reports of the microdistribution of long-circulating liposomes within tumors (24). In marked contrast with anti-HER2 immunoliposomes, intracellular localization of nontargeted liposomes in cancer cells was a rare event. The accumulation of nontargeted liposomes in macrophages, however, was extremely high, with the amount of silver grains per cell too numerous to count.

As a further control, gold-labeled immunoliposomes or nontargeted liposomes were administered i.v. in the MCF-7 breast cancer xenograft model, which lacks HER2 gene amplification and expresses HER2 at low or basal levels ($\sim 10^4$ HER2 receptors/cell; immunohistochemistry score "1+"; ref. 26). The microdistribution of immunoliposomes in MCF-7 xenograft tissue was identical to that of nontargeted liposomes, showing only stromal and macrophage accumulation and virtually no tumor cell internalization (Fig. 3*C*). The mononuclear cells accumulating both HER2-targeted and nontargeted liposomes were confirmed to be macrophages by cytochemical staining for the monocyte marker, nonspecific esterase (Fig. 3*D*). In contrast, anti-HER2 immunoliposomes in BT-474 tumors were observed within tumor cells lacking nonspecific esterase staining (Fig. 3*E*). Thus, in the absence of tumor targeting, either due to the absence of MAb fragments (nontargeted liposomes) or due to insufficient antigen expression (anti-HER2 immunoliposomes in MCF-7 tumors), liposomes could accumulate to high levels in tumor tissue but fail to associate directly with cancer cells.

Cellular analysis of systemically treated tumors. To provide quantitative assessment of this targeting effect, we did two-color

ex vivo flow cytometry to measure the uptake of liposomes/immunoliposomes by tumor or stromal cells in systemically treated tumors. Following i.v. treatment, tumors were disaggregated and suspended, and populations of human carcinoma cells were distinguished from host/murine stromal cells via cytometric detection of HEA (EpCAM; ref. 27; Fig. 4) The extent of *in vivo* uptake of liposomes or immunoliposomes in these respective cell populations was then determined by flow cytometric quantitation of fluorochrome ADS645WS stably encapsulated in liposomes/immunoliposomes.

This assay clearly delineated two distinct cell populations in BT-474 xenografts: EpCAM(+) carcinoma cells and EpCAM(−) stromal cells (Fig. 4*A*). Forty-four hours after i.v. injection of fluorescently labeled liposomes or immunoliposomes, the EpCAM(+) tumor cell population showed a noticeable shift in fluorescence in the case of immunoliposomes, but showed a minimal shift with nontargeted liposomes. In the EpCAM(−) cell population, fluorescence uptake was comparably low in both liposome- and immunoliposome-treated animals (Fig. 4*B* and *C*). Observations of the event density (frequency) profiles of EpCAM and liposome signal intensity on two-dimensional graphs (Fig. 4*D-F*) indeed showed two distinct populations with high or low EpCAM staining. In animals receiving i.v. nontargeted liposomes, the liposome signal was distributed evenly between these two populations (Fig. 4*D*). In contrast, in animals receiving i.v. immunoliposomes, there was a pronounced shift of the EpCAM(+) population into higher immunoliposome signal (Fig. 4*E*).

To distinguish intracellular versus surface uptake in tumor cells, confocal microscopy was done on the same samples (Fig. 4*G* and *H*). This analysis demonstrated that in cells showing positive staining with anti-EpCAM-FITC (i.e., in cancer cells), immunoliposomes were indeed internalized, whereas nontargeted liposomes showed minimal internalization. EpCAM-negative cells containing immunoliposomes or liposomes in high amounts were also observed, consistent with liposome-laden macrophages seen in histologic studies (Fig. 3).

Finally, the flow cytometric assay enabled quantitative analysis of the differential uptake of liposomes versus immunoliposomes in tumor cells versus host/murine cells following i.v. treatment of BT-474 tumor xenografts (Table 3). Immunoliposome delivery achieved true tumor cell targeting: mean immunoliposome-associated fluorescence in tumor cells was greater than in host stromal cells by a factor of 4-fold (P = 0.005). With nontargeted liposome treatment, liposome-associated fluorescence was comparable in cancer cells and host cells (cancer/host ratio of 1.5-fold; P = 0.18), indicating no selectivity for tumor cells. Comparison of tumor cell internalization following treatment with immunoliposomes or liposomes showed an almost 6-fold greater targeting of cancer cells by immunoliposomes, whereas the uptake of immunoliposomes by host cells increased only ~2-fold compared

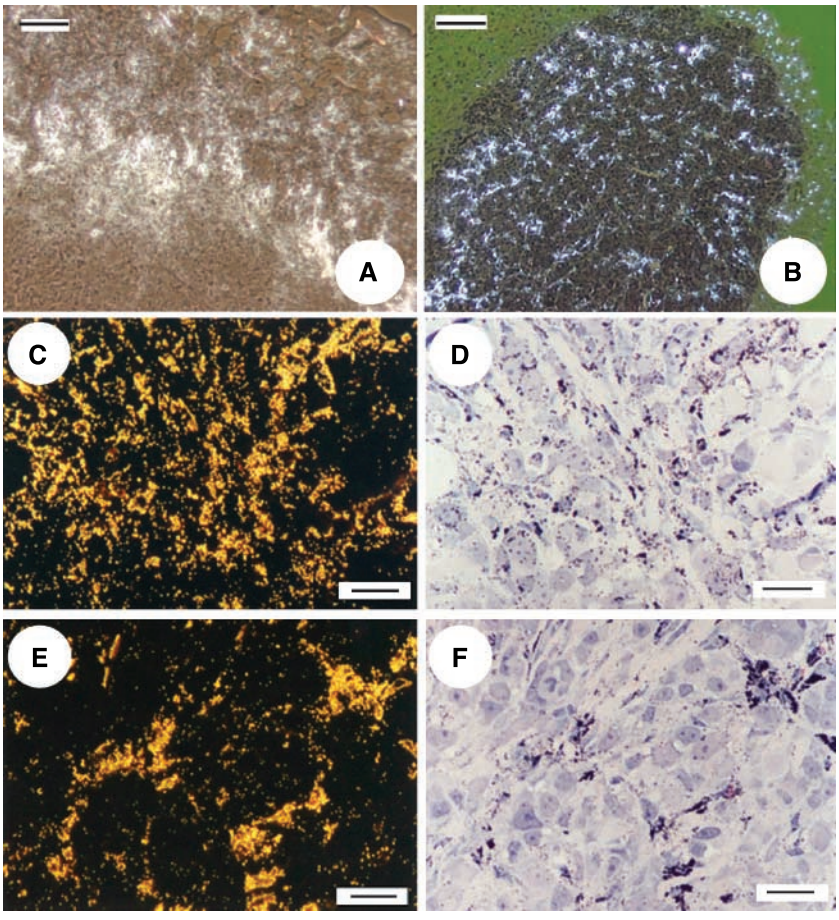

Figure 2. Microdistribution of anti-HER2 immunoliposomes (Fab′ targeted) versus control pegylated liposomes in BT-474 breast cancer xenografts in nude mice. Forty-eight hours following i.v. injection, liposomes/immunoliposomes were visualized in tumor sections by silver enhancement of liposome-encapsulated colloidal gold, and appeared as bright dots on dark-field illumination microscopy (*A*, *B*, *C*, and *E*) or as black grains on bright-field microscopy (*D* and *F*). *A* and *B*, localization of anti-HER2 immunoliposomes (*A*) or control liposomes (*B*) in BT-474 tumors at low-power magnification (×4 objective; *bar*, 250 μm/L). Note the somewhat higher concentrations of liposomes at the interface between the tumor core and periphery. *C-F*, intermediate magnification (×40 objective; *bar*, 25 μm/L) of immunoliposome and liposome localization in BT-474 tumors. Anti-HER2 immunoliposomes showed extensive distribution within tumors (*C*, dark field; *D*, bright field). Control liposomes showed high accumulation but patchy distribution in these tumors (*E*, dark field; *F*, bright field).

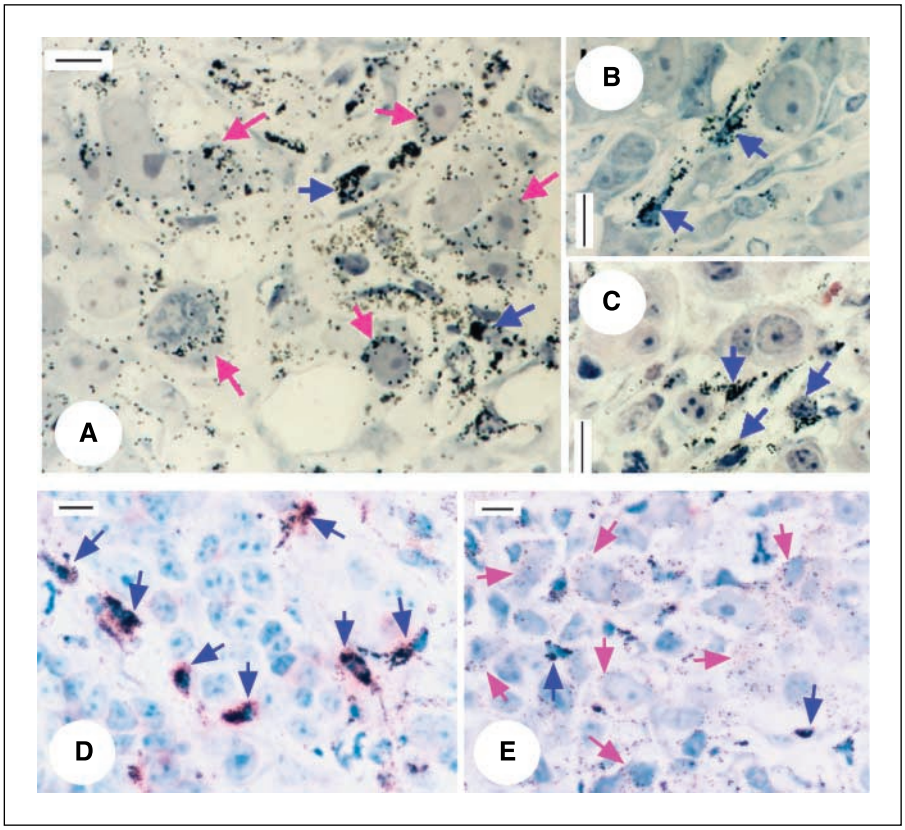

Figure 3. Detailed histologic analysis of the cellular internalization of anti-HER immunoliposomes (Fab′ targeted) versus control pegylated liposomes in breast cancer xenografts in nude mice. Colloidal gold-encapsulating immunoliposomes/liposomes were administered i.v. in nude mice bearing either HER2-overexpressing BT-474 tumors (*A, B*, and *E*) or nonoverexpressing MCF-7 tumors (*C* and *D*). Forty-eight hours postinjection, tumors were excised and colloidal gold was visualized by silver enhancement. At high-power magnification (×100 objective; *bar,* 10 μm/L), cancer cells could be identified as large cells, often in clusters, with large nuclei and prominent nucleoli (*magenta arrows*). Macrophages could be identified as smaller, elongated, or pyramidal cells, typically within stromal gaps, with small densely stained nuclei (*blue arrows*). *A-C,* high-power magnification of immunoliposome and liposome uptake in cells within BT-474 or MCF-7 tumors. *A,* anti-HER2 immunoliposomes showed marked internalization in BT-474 tumor cells and in macrophages. *B,* nontargeted liposomes showed internalization only in macrophages within BT-474 tumor tissue, with minimal tumor cell uptake. *C,* anti-HER2 immunoliposomes showed internalization only in macrophages within MCF-7 tumor tissue, with minimal tumor cell uptake in this HER2-low tumor. *D-E,* high-power magnification with cytochemical staining of macrophages in MCF-7 or BT-474 tumor tissue from animals injected with anti-HER2 immunoliposomes. Macrophages were stained for nonspecific esterase activity (*red*) and tissue was counterstained with Gill's hematoxylin. Immunoliposomes were confirmed to be restricted to macrophage uptake in HER2-low MCF-7 tumors (*D*), but in contrast, had predominantly internalized within tumor cells in HER2-overexpressing BT-474 tumors (*E*).

with nontargeted liposomes. Because these measurements were obtained at a single time point (44 hours posttreatment) following one injection, this 6-fold increase in tumor cell uptake of immunoliposomes represents a robust therapeutic advantage in terms of total intracellular drug exposure. We cannot exclude that the higher doses used in the microdistribution studies may have altered the precise ratio of internalized versus noninternalized liposomes/immunoliposomes as compared with the therapy studies, perhaps decreasing this difference at higher doses due to greater nonspecific uptake.

Discussion

Anti-HER2 immunoliposomes were designed to achieve targeted intracellular delivery to HER2-overexpressing tumor cells. This design has several key features. First, immunoliposomes were rendered long-circulating by modifications including steric stabilization with a PEG-lipid conjugate. Second, the conjugation of multiple antibody fragments was achieved without compromising the pharmacokinetics or biodistribution of long-circulating liposomes. Antibody fragments Fab′ and scFv, rather than intact immunoglobulins, were used to minimize immunogenicity and to circumvent clearance via Fc receptor–mediated mechanisms. Finally, immunoliposomes were optimized for internalization in target cells, including the use of Fab′ fragments from trastuzumab (28) or scFv F5 independently selected based on internalization ability in HER2-overexpressing cells (8). MAb fragments were also positioned distally from the liposome-grafted PEG layer to allow unhindered interaction with the target (6, 29).

We have previously reported that targeted delivery of doxorubicin via anti-HER2 immunoliposomes produced significantly enhanced antitumor efficacy in multiple HER2-overexpressing breast cancer xenograft models as compared with all other treatments tested, including liposomal doxorubicin lacking MAb fragments and the commercial preparation of pegylated liposomal doxorubicin (Doxil; ref. 4). Thus, targeting conferred substantial therapeutic advantage over nontargeted liposomal drug delivery. The present study now provides direct experimental evidence for a distinct mechanism for this enhanced efficacy, i.e., specific association of anti-HER2 immunoliposomes within HER2-overexpressing cancer cells rather than extracellular accumulation within tumor tissue.

Antibody-based agents for cancer therapy, either MAbs themselves ("naked MAbs") or immunoconjugates, have been proposed to provide selective, increased tumor localization due to antibody binding. Contrary to this paradigm, tumor tissue accumulation of immunoliposomes was not significantly increased by MAb targeting, even though immunoliposomes treatment was associated with superior antitumor efficacy over nontargeted liposomes. This result is consistent with the following model for macromolecular agents such as liposomes or other nanoparticles: the rate-limiting step for their tumor localization is extravasation

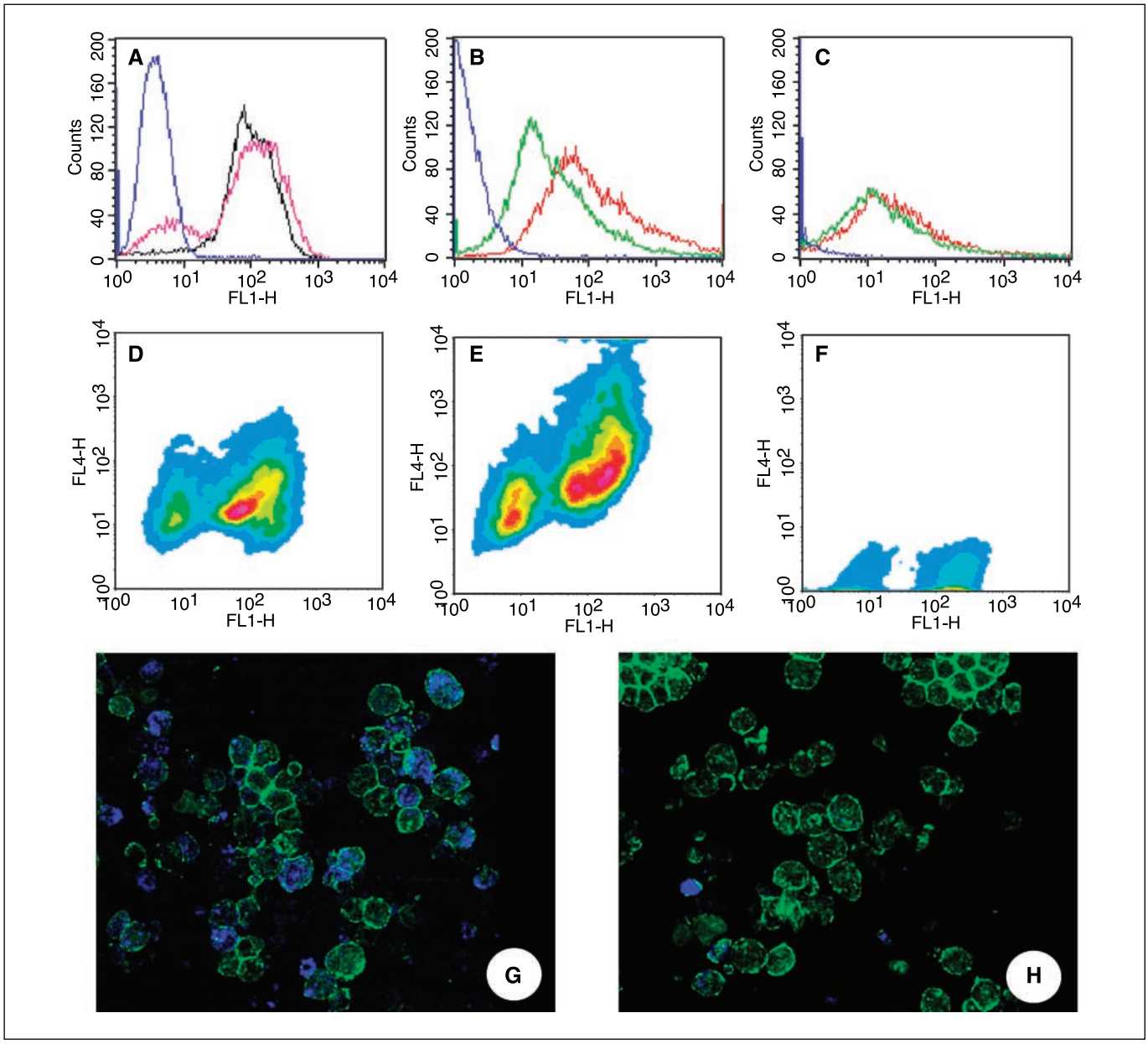

Figure 4. Flow cytometric and confocal fluorescence microscopic analyses of cells obtained from disaggregated s.c. BT-474 xenografts following i.v. injection of liposomes or anti-HER2 immunoliposomes (scFv F5-targeted). *A,* disaggregated BT-474 xenografts were stained for HEA (EpCAM) expression using anti-EpCAM MAb-FITC conjugate, demonstrating two distinct peaks (*magenta line*): EpCAM(+) carcinoma cells and EpCAM(−) host (murine) cells. As a control, BT-474 cells grown in culture were similarly stained, and appeared as a single peak (*black line*) corresponding with the EpCAM(+) cells harvested from disaggregated tumors. *Blue line,* unstained cells (autofluorescence control). *B* and *C,* liposomes or immunoliposomes containing encapsulated fluorescent marker, ADS645WS, were administered i.v. in BT-474 xenograft-bearing nude mice; 44 hours postinjection, tumors were disaggregated and analyzed by flow cytometry for anti-EpCAM MAb-FITC (to distinguish tumor versus host cells) and ADS645WS. Gating on the EpCAM(+) cell population (*B*) showed a clear shift indicating higher uptake of immunoliposomes (*red line*) as compared with nontargeted liposomes (*green line*). In contrast, gating on the EpCAM(−) cell population (*C*) showed equivalent and low uptake for both liposomes and immunoliposomes. *Blue lines,* tumor samples obtained from animals which received saline only (autofluorescence controls). *D-F,* two-dimensional event density plots of disaggregated tumor cell suspensions from animals injected with ADS645WS-labeled anti-HER2 immunoliposomes (*E*), control liposomes (*D*), or saline (*F*). Liposome label fluorescence was recorded in channel FL4-H and anti-EpCAM MAb-FITC fluorescence in channel FL1-H. Relative event density is color-coded as follows: *blue* (1-5%); *light blue* (5–15%), *green* (15-30%), *yellow-green* (30-45%), *yellow* (45-60%), *orange* (60-75%), *red* (75-90%), and *magenta* (90-100%). Note the shift to higher FL4 values in the FL1-gated cell population in animals injected with immunoliposomes as opposed to liposomes, in which there is no such shift. *G* and *H,* confocal microscopy of tumor cell suspensions obtained from mice injected with anti-HER2 immunoliposomes (*G*) or control liposomes (*H*). Liposomes/immunoliposomes were labeled with encapsulated ADS645WS (*blue*); tumor cells were counterstained with anti-EpCAM MAb-FITC conjugate (*green*). Magnification, ×400.

Table 3. Flow cytometric analysis of uptake of immunoliposomes versus liposomes in cancer cells (EpCAM-positive) versus mouse host cells (EpCAM-negative) recovered from HER2-overexpressing BT-474 tumor xenografts in nude mice 44 hours after i.v. injection

Injected formulation	Cancer cells (EpCAM+)	Host/mouse cells (EpCAM−)	Ratio, cancer/host	*P*, tumor vs. host
Liposomes	74.1 ± 25.0	49.4 ± 4.1	1.5	0.1838
Anti-HER2 immunoliposomes	392.3 ± 84.4	98.3 ± 11.6	4.1	0.00843
Control (no treatment)	9.1 ± 4.7	4.9 ± 0.9	not done	0.3275
Ratio, immunoliposomes/liposomes	5.9	2.1		
P, immunoliposomes vs. liposomes	0.00503	0.00298		

NOTE: Data represent mean fluorescence ±SD of the indicated treatment groups (n = 4 per group). P values were calculated using nonpaired two-tailed Student's t test.

from tumor vasculature, and this is driven by factors such as circulation time and particle size. MAb-antigen interactions do not necessarily facilitate this process. Rather, both anti-HER2 immunoliposomes and nontargeted liposomes equally benefited from the "enhanced permeability and retention" (EPR) effect, in which long-circulating agents undergo preferential extravasation at sites of abnormal tumor vessel microanatomy associated with tumor angiogenesis, and combined with deficient tumor lymphatics leads to "passive targeting" or accumulation in tumors (30). Preclinical (31, 32) and clinical studies (33) previously showed that long-circulating liposomes do in fact preferentially accumulate in tumors as predicted by the EPR effect. Indeed, the efficiency of tumor localization observed for both targeted and nontargeted liposomes in this study (7-8% injected dose/g at 24 hours) was superior to that of free anti-HER2 MAb in similar models (34). The lack of increased tumor accumulation of alternatively designed anti-HER2 immunoliposomes as compared with nontargeted sterically stabilized liposomes has been previously reported (35). However, in these studies, antibody-directed targeting also did not result in therapeutic gain, possibly because of insufficient immunoliposome internalization.

The mechanism of anti-HER2 immunoliposome-mediated drug delivery is novel and distinct from that associated with drug delivery by nontargeted liposomes. Nontargeted sterically stabilized liposomes have been shown to accumulate in perivascular areas and adjacent extracellular space; eventually, liposome breakdown or phagocytic uptake could occur, resulting in the release of encapsulated drug for subsequent diffusion to nearby cancer cells (31). The studies in this report confirmed that nontargeted liposomes act by efficient tumor extravasation followed by accumulation in tumor stroma, including the extracellular space and within tumor-associated macrophages. In contrast, anti-HER2 immunoliposomes, after equally efficient extravasation, predominantly accumulated within the cytoplasm of HER2-overexpressing tumor cells, indicating that binding and internalization of immunoliposomes in tumor cells occurs *in vivo* as well as *in vitro*. The internalization of anti-HER2 immunoliposomes was previously shown to be mediated by the MAb fragment, as immunoliposomes bearing irrelevant MAb fragments failed to bind or internalize in HER2-overexpressing cancer cells *in vitro* (5). To our knowledge, this is the first direct demonstration of immunoliposome-mediated intracellular drug delivery in tumor cells *in vivo*.

How does the internalization of drug-carrying immunoliposomes in tumor cells enhance therapeutic efficacy against solid tumors? One explanation is that internalization leads to the intracellular release of bioactive drug near its subcellular site(s) of action. In the case of doxorubicin, acidification of the immunoliposome milieu upon receptor-mediated endocytosis would lead to drug release into the endolysosomal compartment, followed by rapid permeation of doxorubicin into the cytosol and nucleus. Redistribution of doxorubicin and other weak lipophilic bases across lipid membranes towards acidic pH is well-established; for example, the efflux of doxorubicin from liposomes into acidified medium has been directly shown (36). Another possibility is that MAb-targeting of immunoliposomes may facilitate better tumor penetration; this is supported by the more extensive distribution of immunoliposomes as compared with liposomes when visualized in tumor tissue. Although uptake by tumor-resident macrophages has been proposed as a mechanism for drug release from sterically stabilized liposomes (37), this mechanism seems to be less direct and less efficient than intracellular release within tumor cells. Hence, although immunoliposome delivery did not quantitatively increase drug levels in tumor tissue, it qualitatively altered the mechanism of delivery to tumor cells for enhanced activity.

In conclusion, we have shown a distinct mechanism for immunoliposomal drug delivery to tumor cells *in vivo*. This mechanism does not involve increased tumor localization, which was due to the EPR effect, but rather exploits antibody-dependent binding and internalization in tumor cells. These results may have implications for other nanoparticle-based agents containing MAb fragments or other ligands, and suggest that such approaches should be engineered for efficient internalization. Anti-HER2 immunoliposomes capable of penetrating tumor tissue, internalizing specifically in HER2-overexpressing cancer cells and intracellularly releasing encapsulated drugs represent a potentially advantageous strategy for molecularly targeted drug delivery.

Acknowledgments

Received 11/23/2005; revised 3/26/2006; accepted 4/13/2006.

Grant support: The National Cancer Institute (NIH P50 CA 58207-01, NIH P50 CA CA097257, and NIH U54 CA90788).

The costs of publication of this article were defrayed in part by the payment of page charges. This article must therefore be hereby marked *advertisement* in accordance with 18 U.S.C. Section 1734 solely to indicate this fact.

The authors thank Dr. Ann Thor for helpful discussions, Dr. Eric Beattie for assistance with confocal microscopy, and Ilse Sauerwald for expert technical assistance.

References

1. Allen TM, Cullis PR. Drug delivery systems: entering the mainstream. Science 2004;303:1818–22.
2. Drummond DC, Meyer O, Hong K, Kirpotin DB, Papahadjopoulos D. Optimizing liposomes for delivery of chemotherapeutic agents to solid tumors. Pharmacol Rev 1999;51:691–743.
3. Noble CO, Kirpotin DB, Hayes ME, et al. Development of ligand-targeted liposomes for cancer therapy. Expert Opin Ther Targets 2004;8:335–53.
4. Park JW, Hong K, Kirpotin DB, et al. Anti-HER2 immunoliposomes: enhanced efficacy attributable to targeted delivery. Clin Cancer Res 2002;8:1172–81.
5. Park JW, Hong K, Carter P, et al. Development of anti-p185HER2 immunoliposomes for cancer therapy. Proc Natl Acad Sci U S A 1995;92:1327–31.
6. Kirpotin D, Park JW, Hong K, et al. Sterically stabilized anti-HER2 immunoliposomes: design and targeting to human breast cancer cells *in vitro*. Biochemistry 1997; 36:66–75.
7. Carter P, Rodrigues ML, Park JW, Zapata G. Preparation and uses of Fab′ fragments from *E. coli*. In: McCafferty J, Hoogenboom HR, Chiswell D, editors. Antibody engineering: a practical approach. Oxford, UK: IRL Press; 1996. p. 291–308.
8. Poul MA, Becerril B, Nielsen UB, Morisson P, Marks JD. Selection of tumor-specific internalizing human antibodies from phage libraries. J Mol Biol 2000;301:1149–61.
9. Nielsen UB, Kirpotin DB, Pickering EM, et al. Therapeutic efficacy of anti-ErbB2 immunoliposomes targeted by a phage antibody selected for cellular endocytosis. Biochim Biophys Acta 2002;1591:109–18.
10. Nellis DF, Giardina SL, Janini GM, et al. Preclinical manufacture of anti-HER2 liposome-inserting, scFv-PEG-lipid conjugate. 2. Conjugate micelle identity, purity, stability, and potency analysis. Biotechnol Prog 2005;21:221–32.
11. Nellis DF, Ekstrom DL, Kirpotin DB, et al. Preclinical manufacture of an anti-HER2 scFv-PEG-DSPE, liposome-inserting conjugate. 1. Gram-scale production and purification. Biotechnol Prog 2005;21:205–20.
12. Woodle MC. ^{67}Gallium-labeled liposomes with prolonged circulation: preparation and potential as nuclear imaging agents. Nucl Med Biol 1993;20:149–55.
13. Hong K, Friend DS, Glabe CG, Papahadjopoulos D. Liposomes containing colloidal gold are a useful probe of liposome-cell interactions. Biochim Biophys Acta 1983;732:320–3.
14. Szoka F, Papahadjopoulos D. Procedure for preparation of liposomes with large internal aqueous space and high capture by reverse-phase evaporation. Proc Natl Acad Sci U S A 1978;75:4194–8.
15. Brunetti A, Blasberg RG, Finn RD, Larson SM. Gallium-transferrin as a macromolecular tracer of vascular permeability. Int J Rad Appl Instrum B 1988; 15:665–72.
16. Kirpotin DB, Shao Y, Stauffer P, et al. Local hyperthermia facilitates inmmunoliposome targeting to breast cancer xenografts [abstract 2069]. Proc Am Assoc Cancer Res 2002;43:416.
17. Carter P, Presta L, Gorman C, et al. Humanization of an anti-p185HER2 antibody for human cancer therapy. Proc Natl Acad Sci U S A 1992;89:4285–9.
18. Mamot C, Drummond DC, Noble CO, et al. Epidermal growth factor receptor-targeted immunoliposomes significantly enhance the efficacy of multiple anticancer drugs *in vivo*. Cancer Res 2005;65:11631–8.
19. Otsuki H, Brunetti A, Owens ES, Finn RD, Blasberg RG. Comparison of iron-59, indium-111, and gallium-69 transferrin as a macromolecular tracer of vascular permeability and the transferrin receptor. J Nucl Med 1989;30:1676–85.
20. Papahadjopoulos D, Allen TM, Gabizon A, et al. Sterically stabilized liposomes: improvements in pharmacokinetics and antitumor therapeutic efficacy. Proc Natl Acad Sci U S A 1991;88:11460–4.
21. Maruyama K, Takahashi N, Ishida O, Iwatsuru M. Construction of transferrin-PEG-liposomes for intracellular drug delivery in solid tumors *in vivo*. J Liposome Res 1998;8:81–2.
22. Damert A, Machein M, Breier G, et al. Up-regulation of vascular endothelial growth factor expression in a rat glioma is conferred by two distinct hypoxia-driven mechanisms. Cancer Res 1997;57:3860–4.
23. Takano S, Yoshii Y, Kondo S, et al. Concentration of vascular endothelial growth factor in the serum and tumor tissue of brain tumor patients. Cancer Res 1996; 56:2185–90.
24. Huang SK, Lee K-D, Hong K, Friend DS, Papahadjopoulos D. Microscopic localization of sterically stabilized liposomes in colon carcinoma-bearing mice. Cancer Res 1992; 52:5135–43.
25. Yuan F, Lwunig M, Huang SK, Berk DA, Papahadjopoulos D, Jain RK. Microvascular permeability and interstitial penetration of sterically stabilized (stealth) liposomes in a human tumor xenograft. Cancer Res 1994;54: 3352–6.
26. Lewis GD, Figari I, Fendly B, et al. Differential responses of human tumor cell lines to anti-p185HER2 monoclonal antibodies. Cancer Immunol Immunother 1993;37:255–63.
27. Moldenhauer G, Momburg F, Moller P, Schwartz R, Hammerling GJ. Epithelium-specific surface glycoprotein of M_r 34,000 is a widely distributed human carcinoma marker. Br J Cancer 1987;56:714–21.
28. Sarup JC, Johnson RM, King KL, et al. Characterization of an anti-p185HER2 monoclonal antibody that stimulates receptor function and inhibits tumor cell growth. Growth Regul 1991;1:72–82.
29. Allen TM, Brandeis E, Hansen CB, Kao GY, Zalipsky S. A new strategy for attachment of antibodies to sterically stabilized liposomes resulting in efficient targeting to cancer cells. Biochim Biophys Acta 1995;1237:99–108.
30. Noguchi Y, Wu J, Duncan R, et al. Early phase tumor accumulation of macromolecules: a great difference in clearance rate between tumor and normal tissues. Jpn J Cancer Res 1998;89:307–14.
31. Huang SK, Mayhew E, Gilani S, Lasic DD, Martin FJ, Papahadjopoulos D. Pharmacokinetics and therapeutics of sterically stabilized liposomes in mice bearing C-26 colon carcinoma. Cancer Res 1992;52:6774–81.
32. Gabizon A, Goren D, Horowitz AT, Tzemach D, Lossos A, Siegal T. Long-circulating liposomes for drug delivery in cancer therapy: a review of biodistribution studies in tumor-bearing animals. Adv Drug Deliv Rev 1997;24:337–44.
33. Northfelt DW, Martin FJ, Working P, et al. Doxorubicin encapsulated in liposomes containing surface-bound polyethylene glycol: pharmacokinetics, tumor localization, and safety in patients with AIDS-related Kaposi's sarcoma. J Clin Pharmacol 1996;36:55–63.
34. Park JW, Stagg R, Lewis GD, et al. Anti-p185HER2 monoclonal antibodies: biological properties and potential for immunotherapy. In: Dickson RB, Lippman ME, editors. Genes, oncogenes, and hormones: advances in cellular and molecular biology of breast cancer. Boston: Kluwer; 1992. p. 193–211.
35. Goren D, Horowitz AT, Zalipsky S, Woodle MC, Yarden Y, Gabizon A. Targeting of stealth liposomes to erbB-2 (Her/2) receptor: *in vitro* and *in vivo* studies. Br J Cancer 1996;74:1749–56.
36. Lee RJ, Wang S, Turk MJ, Low PS. The effects of pH and intraliposomal buffer strength on the rate of liposome content release and intracellular drug delivery. Biosci Rep 1998;18:69–78.
37. Vail DM, Amantea MA, Colbern GT, Martin FJ, Hilger RA, Working PK. Pegylated liposomal doxorubicin: proof of principle using preclinical animal models and pharmacokinetic studies. Semin Oncol 2004;31:16–35.